A Meshfree Semi-implicit Smoothed Particle Hydrodynamics Method for Free Surface Flow

Adeleke O. Bankole, Michael Dumbser, Armin Iske, and Thomas Rung

Abstract This work concerns the development of a meshfree semi-implicit numerical scheme based on the Smoothed Particle Hydrodynamics (SPH) method, here applied to free surface hydrodynamic problems governed by the shallow water equations. In *explicit* numerical methods, a severe limitation on the time step is often due to stability restrictions imposed by the CFL condition. In contrast to this, we propose a *semi-implicit* SPH scheme, which leads to an unconditionally stable method. To this end, the discrete momentum equation is substituted into the discrete continuity equation to obtain a linear system of equations for only one scalar unknown, the free surface elevation. The resulting system is not only sparse but moreover symmetric positive definite. We solve this linear system by a matrix-free conjugate gradient method. Once the new free surface location is known, the velocity can directly be computed at the next time step and, moreover, the particle positions can subsequently be updated. The resulting meshfree semi-implicit SPH method is validated by using a standard model problem for the shallow water equations.

A.O. Bankole • A. Iske (✉)
Department of Mathematics, University of Hamburg, Bundesstrasse 55, 20146 Hamburg, Germany
e-mail: adeleke.bankole@uni-hamburg.de; armin.iske@uni-hamburg.de; iske@math.uni-hamburg.de

M. Dumbser
Department of Civil, Environmental and Mechanical Engineering, University of Trento, Via Mesiano 77, I-38123 Trento, Italy
e-mail: michael.dumbser@unitn.it

T. Rung
Institute of Fluid Dynamics and Ship Theory, Hamburg University of Technology, Am Schwarzenberg-Campus 4, 21073 Hamburg, Germany
e-mail: thomas.rung@tuhh.de

M. Griebel, M.A. Schweitzer (eds.), *Meshfree Methods for Partial Differential Equations VIII*, Lecture Notes in Computational Science and Engineering 115,
DOI 10.1007/978-3-319-51954-8_3

1 Introduction

In this work, we propose a meshfree semi-implicit SPH scheme for two-dimensional inviscid hydrostatic free surface flows. These flows are governed by the *shallow water equations* which can be derived either vertically or laterally averaged from the three dimensional incompressible Navier-Stokes equations with the assumption of a hydrostatic pressure distribution (see [5, 6]).

Several methods have been developed for both structured and unstructured meshes using finite difference, finite volume and finite element schemes [5–8, 19]. Explicit schemes are often limited by a severe time step restriction, due to the Courant-Friedrichs-Lewy (CFL) condition. In contrast, semi-implicit methods lead to stable discretizations allowing large time steps at reasonable computational costs. In staggered grid methods for finite differences and finite volumes, discrete variables are often defined at different (staggered) locations. The pressure term, which is the free surface elevation, is defined in the cell center, while the velocity components are defined at the cell interfaces. In the momentum equation, both the pressure term, due to the gradients in the free surface elevations, and the velocity term, in the mass conservation, are discretized implicitly, whereas the nonlinear convective terms are discretized explicitly. In mesh-based schemes, the semi-Lagrangian method discretizes these terms explicitly (see [3, 12, 13]).

In this work a new semi-implicit *Smoothed Particle Hydrodynamics* (SPH) scheme for the numerical solution of the shallow water equations in two space dimensions is proposed, where the flow variables are the particle free surface elevation, the particle total water depth, and the particle velocity. The discrete momentum equations are substituted into the discretized mass conservation equation to give a discrete equation for the free surface leading to a system in only one single scalar quantity, the free surface elevation location. Solving for one scalar quantity in a single equation distinguishes our method, in terms of efficiency, from other methods. The system is solved for each time step as a linear algebraic system. The components of the momentum equation at the new time level can directly be computed from the new free surface, which we conveniently solve by a matrix-free version of the conjugate gradient (CG) algorithm [11, 17]. Consequently, the particle velocities are computed at the new time step and the particle positions are then updated. In this semi-implicit SPH method, the stability is independent of the wave celerity. Therefore, large time steps can be permitted to enhance the numerical efficiency [5].

The rest of this paper is organized as follows. The problem formulation, including the two-dimensional shallow water equations and the utilized models for the particle approximations, is given in Sect. 2. Our meshfree semi-implicit SPH scheme is constructed in Sect. 3. Numerical results, to validate the proposed semi-implicit SPH scheme, are presented in Sect. 4. Concluding remarks are given in Sect. 5.

2 Problem Formulation and Models

This section briefly introduces the utilized models and particle approximations. Vectors are defined by reference to Cartesian coordinates. Latin subscripts are used to identify particle locations, where subscript i refers to the focal particle and subscript j denotes the neighbor of particle i.

2.1 The Kernel Function

We use a mollifying function W, a positive decreasing radially symmetric function with compact support, of the generic form

$$W(r,h) = \frac{1}{h^d} W\left(\frac{\|r\|}{h}\right) \quad \text{for} \quad r \in [0,\infty) \quad \text{and} \quad h > 0.$$

In our numerical examples, we work with the B-spline kernel of degree 3 [15], given as

$$W(r,h) = W_{ij} = K \times \begin{cases} 1 - \frac{3}{2}\left(\frac{r}{h}\right)^2 + \frac{3}{4}\left(\frac{r}{h}\right)^3 & \text{for} \quad 0 \le \frac{r}{h} \le 1 \\ \frac{1}{4}\left(2 - \frac{r}{h}\right)^3 & \text{for} \quad 1 \le \frac{r}{h} \le 2 \\ 0 & \text{for} \quad \frac{r}{h} > 2 \end{cases}$$

where the normalisation coefficient K takes the value $2/3$ (for dimension $d = 1$), $10/(7\pi)$ (for $d = 2$), or $1/\pi$ (for $d = 3$). For the mollifier $W \in W^{3,\infty}(\mathbb{R}^d)$, $h > 0$ is referred to as the *smoothing length*, being related to the particle spacing Δ_P by $h = 2\Delta_P$. The smoothing length h can vary locally according to

$$h_{ij} = \frac{1}{2}[h_i + h_j] \qquad \text{where } h_i = \sigma \sqrt[d]{\frac{m_j}{\rho_j}}. \tag{1}$$

In this study, we use the smoothing length in (1). Moreover, σ is in $[1.5, 2.0]$, which ensures approximately a constant number of particle neighbors of between 40–50 in the compact support of each kernel. A popular approach for the kernel's normalisation is by Shepard interpolation [18], where

$$W'_{ij} = \frac{W_{ij}}{\sum_{j=1}^{N} \frac{m_j}{\rho_j} W_{ij}}.$$

Normalisation is of particular importance for particles close to free surfaces, since this will reduce numerical instabilities and other undesired effects near the boundary.

The gradient of the kernel function is corrected by using the formulation proposed by Belytschko et al. [1]. For the sake of notational convenience, we will from now refer to the kernel function W'_{ij} as W_{ij} and to its gradient $\nabla W'_{ij}$ as ∇W_{ij}.

2.2 Governing Equations

The governing equations considered in this work are nonlinear hyperbolic conservation laws of the form

$$L_b(\mathbf{\Phi}) + \nabla \cdot (\boldsymbol{F}(\mathbf{\Phi}, \boldsymbol{x}, t)) = 0 \qquad \text{for } t \in \mathbb{R}^+, \mathbf{\Phi} \in \mathbb{R} \tag{2}$$

together with the initial condition

$$\mathbf{\Phi}(\boldsymbol{x}, 0) = \mathbf{\Phi}_0(\boldsymbol{x}) \qquad \text{for } \boldsymbol{x} \in \Omega \subset \mathbb{R}^d, \mathbf{\Phi}_0 \in \mathbb{R}$$

where L_b is the transport operator given by

$$L_b(\mathbf{\Phi}) = \frac{\partial \mathbf{\Phi}}{\partial t} + \nabla \cdot (b\mathbf{\Phi})$$

and

$$\boldsymbol{x} = (x^1, \ldots, x^d), \quad \boldsymbol{F} = (F^1, \ldots, F^d), \quad \boldsymbol{b} = (b^1, \ldots, b^d),$$

where $\boldsymbol{b}$ is a regular vector field in $\mathbb{R}^d$, $\boldsymbol{F}$ is a flux vector in $\mathbb{R}^d$, and $\boldsymbol{x}$ is the position.

Figure 1 gives a sketch of the flow domain, i.e., the free surface elevation and the bottom bathymetry. In this configuration, the vertical variation is much smaller

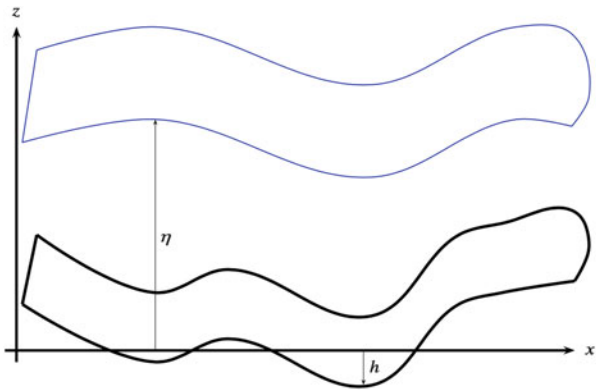

Fig. 1 Sketch of the flow domain: the free surface (*light*) and the bottom bathymetry (*thick*)

than the horizontal variation, as typical for rivers flowing over long distances of e.g. hundreds or thousands of kilometers. We consider the frictionless, inviscid two dimensional shallow water equations in Lagrangian derivatives, given as

$$\frac{D\eta}{Dt} + \nabla \cdot (H\boldsymbol{v}) = 0 \tag{3}$$

$$\frac{D\boldsymbol{v}}{Dt} + g\nabla\eta = 0 \tag{4}$$

$$\frac{D\boldsymbol{r}}{Dt} = \boldsymbol{v} \tag{5}$$

where $\eta = \eta(x, y, t)$ is the free surface location,

$$H(x, y, t) = h(x, y) + \eta(x, y, t)$$

is the total water depth with bottom bathymetry $h(x, y)$, and where $\boldsymbol{v} = v(x, y, t)$ is the particle velocity, $\boldsymbol{r} = r(x, y, t)$ the particle position, and g the gravity acceleration.

2.3 Hydrostatic Approximation

In geophysical flows, the vertical acceleration is often small when compared to the gravitational acceleration and to the pressure gradient in the vertical direction. This is the case in our flow model shown in Fig. 1. If we consider, for instance, tidal flows in the ocean, the velocity in the horizontal direction is of the order of 1 m/s, whereas the velocity in the vertical direction is only of the order of one meter per tidal cycle. Therefore, the advective and viscous terms in the vertical momentum equation of the Navier-Stokes equation are neglected, in which case the pressure equation becomes

$$\frac{dp}{dz} = -g, \tag{6}$$

with normalised pressure, i.e., the pressure is divided by a constant density. The solution of (6) is given by the hydrostatic pressure

$$p(x, y, z, t) = p_0(x, y, t) + g[\eta(x, y, t) - z],$$

where $p_0(x, y, t)$ is the atmospheric pressure at the free surface, taken as constant.

3 Construction of a Meshfree Semi-implicit SPH Scheme

There are several numerical methods for solving Eqs. (3)–(5), including finite differences, finite volumes or finite elements, explicit or implicit methods, conservative or non-conservative schemes, mesh-based or meshfree methods. The meshfree SPH scheme of this work relies on the semi-implicit finite difference method of Casulli [4].

Explicit numerical methods are often, for the sake of numerical stability, limited by the CFL condition. The resulting stability restrictions are usually leading to very small time steps, in contrast to implicit methods. In fact, fully implicit discretisations lead to unconditionally stable methods. On the down side, they typically require solving a large number of coupled nonlinear equations. Moreover, for the sake accuracy, the time step size in implicit methods cannot be chosen arbitrarily large. Semi-implicit methods, e.g. that of Casulli [4], aim to reduce the shortcomings of explicit and fully implicit methods. Following along the lines of [4], we achieve to balance accuracy and stability, at reasonable time step sizes, by a semi-implicit SPH scheme for the two-dimensional shallow water equations, as supported by our numerical results.

3.1 The Smoothed Particle Hydrodynamics Method

Let us briefly recall the basic features of the smoothed particle hydrodynamics (SPH) method. The SPH method is regarded as a powerful tool in computational fluid dynamics. Due to the basic concept of SPH, numerical simulations for fluid flow are obtained by discretisations of the flow equations with using finite sets of particles. Moreover, the target flow quantity, say $A(t, \boldsymbol{x})$, e.g., the velocity field or water height, is smoothed by a suitable kernel function $W(\boldsymbol{x}, \boldsymbol{x}', h)$, by smoothing parameter $h > 0$, w.r.t. the measure that is associated with the mass density $\rho(t, \boldsymbol{x})$ of the flow, i.e.,

$$A(t, \boldsymbol{x}) = \int_{\Omega} \frac{A(t, \boldsymbol{x}')}{\rho(t, \boldsymbol{x}')} W(\boldsymbol{x} - \boldsymbol{x}', h) \rho(t, \boldsymbol{x}') d\boldsymbol{x}' \qquad \text{for } h > 0.$$

Due to the Lagrangian description of SPH, the smoothed quantities are approximated by a set of Lagrangian particles, each carrying an individual mass m_i, density ρ_i and field property A_i. Accordingly, for a given point $\boldsymbol{x}$ in space, the field property A_i, defined at the particles, located at $\boldsymbol{x}_j$, can be interpolated from neighboring points:

$$A(t, \boldsymbol{x}) \approx \sum_{j=1}^{N} m_j \frac{A_j(t)}{\rho_j(t)} W(\boldsymbol{x} - \boldsymbol{x}_j, h),$$

i.e., the field property A at point $\boldsymbol{x}$ is approximated by the sum of contributions from particles at $\boldsymbol{x}_j$ surrounding $\boldsymbol{x}$, being weighted by the distance from each particle. The smoothing kernel $W(\boldsymbol{x}-\boldsymbol{x}', h)$ is required to satisfy the following properties.

- **Unit mass:**

$$\int_\Omega W(\boldsymbol{x}-\boldsymbol{x}', h) d\boldsymbol{x}' = 1 \qquad \text{for all } \boldsymbol{x} \text{ and } h > 0.$$

- **Compact support:**

$$W(\boldsymbol{x}-\boldsymbol{x}', h) = 0 \qquad \text{for } |\boldsymbol{x}-\boldsymbol{x}'| > \alpha h,$$

  where the scaling factor $\alpha > 0$ determines the shape (i.e., flatness) of W.
- **Positivity:**

$$W(\boldsymbol{x}-\boldsymbol{x}', h) \geq 0 \qquad \text{for all } \boldsymbol{x}, \boldsymbol{x}' \text{ and } h > 0.$$

- **Decay:** $W(\boldsymbol{x}-\boldsymbol{x}', h)$ should, for any $h > 0$, be monotonically decreasing.
- **Localisation:**

$$\lim_{h \searrow 0} W(\boldsymbol{x}-\boldsymbol{x}', h) = \delta(\boldsymbol{x}-\boldsymbol{x}') \qquad \text{for all } \boldsymbol{x}, \boldsymbol{x}',$$

  where δ denotes the usual Dirac point evaluation functional.
- **Symmetry:** $W(\boldsymbol{x}-\boldsymbol{x}', h)$ should, for any $h > 0$, be an even function.
- **Smoothness:** W should be sufficiently smooth (yet to be specified).

3.2 Classical SPH Formulation

The standard SPH formulation discretizes the computational domain $\Omega(t)$ by a finite set of N particles, with positions $\boldsymbol{r}_i$. According to Gingold and Monaghan [10], the SPH discretization of the shallow water equations (3)–(5) are given as

$$\frac{\eta_i^{n+1} - \eta_i^n}{\Delta t} + \sum_{j=1}^{N} \frac{m_j}{\rho_j} H_{ij}^n \boldsymbol{v}_j^n \nabla W_{ij} = \boldsymbol{0} \tag{7}$$

$$\frac{\boldsymbol{v}_i^{n+1} - \boldsymbol{v}_i^n}{\Delta t} + g \sum_{j=1}^{N} \frac{m_j}{\rho_j} \eta_j^n \nabla W_{ij} = \boldsymbol{0} \tag{8}$$

$$\frac{\boldsymbol{r}_i^{n+1} - \boldsymbol{r}_i^n}{\Delta t} = \boldsymbol{v}_i^n \tag{9}$$

where the particles are advected by (9), with Δt being the time step size, m_j the particle mass, ρ_j the particle density, and ∇W_{ij} is the gradient of kernel W_{ij} w.r.t. x_i. In the scheme [10, 15] of Gingold and Monaghan, $\nabla \cdot (H\boldsymbol{v})$ and $\nabla \eta$ are explicitly computed. We remark that Eqs. (7)–(9) follow from a substitution of the flow variable with corresponding derivatives, using integration by parts, and the divergence theorem.

3.3 SPH Formulation of Vila and Ben Moussa

In the construction of our proposed semi-implicit SPH scheme, we use the concept of Vila and Ben Moussa [2, 21], whose basic idea is to replace the centered approximation

$$(F(v_i, x_i, t) + F(v_j, x_j, t)) \cdot n_{ij}$$

of (2) by a numerical flux $G(n_{ij}, v_i, v_j)$, from a conservative finite difference scheme, satisfying

$$G(n(x), v, v) = F(v, x, t) \cdot n(x)$$
$$G(n, v, u) = -G(-n, u, v).$$

With using this formalism, the SPH discretization of Eqs. (7)–(8) becomes

$$\frac{\eta_i^{n+1} - \eta_i^n}{\Delta t} + \sum_{j=1}^{N} \frac{m_j}{\rho_j} 2H_{ij}^n \boldsymbol{v}_{ij}^n \nabla W_{ij} = \mathbf{0},$$

$$\frac{\boldsymbol{v}_i^{n+1} - \boldsymbol{v}_i^n}{\Delta t} + g \sum_{j=1}^{N} \frac{m_j}{\rho_j} 2\eta_{ij}^n \nabla W_{ij} = \mathbf{0}.$$

In this way, we define for a pair of particles, i and j, the free surface elevation η_i, η_j and the velocity $\boldsymbol{v}_i$, $\boldsymbol{v}_j$, respectively (see Fig. 2). In our approach, we, moreover,

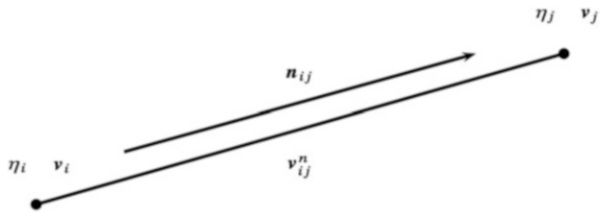

Fig. 2 Staggered velocity defined at the midpoint of two pair of interacting particles i and j

use a staggered velocity $\boldsymbol{v}_{ij}$ between two interacting particles i and j as

$$\boldsymbol{v}_{ij} = \frac{1}{2}(\boldsymbol{v}_i + \boldsymbol{v}_j) \cdot \boldsymbol{n}_{ij}$$

in the normal direction $\boldsymbol{n}_{ij}^{d=1,2}$ at the midpoint of the two interacting particles, where

$$n_{ij}^1 = \frac{x_j - x_i}{\|x_j - x_i\|} \qquad \text{and} \qquad n_{ij}^2 = \frac{y_j - y_i}{\|y_j - y_i\|}$$

for the two components of vector $\boldsymbol{n}_{ij}$. Moreover,

$$\delta_{ij}^1 = \|x_j - x_i\| \qquad \text{and} \qquad \delta_{ij}^2 = \|y_j - y_i\|$$

gives the distance between particles i and j. Since the velocities at the particles' midpoint are known, we can use kernel summation for velocity updates.

3.4 Semi-implicit SPH Scheme

For the derivation of the semi-implicit SPH scheme, let us regard the governing equations (3)–(5). Writing Eqs. (3)–(5) in a non-conservative quasi-linear form by expanding derivatives in the continuity equation and momentum equations (with assuming smooth solutions), this yields

$$u_t + uu_x + vu_y + g\eta_x = 0 \tag{10}$$

$$v_t + uv_x + vv_y + g\eta_y = 0 \tag{11}$$

$$\eta_t + u\eta_x + v\eta_y + H(u_x + v_y) = -uh_x - vh_y. \tag{12}$$

Rewriting (10)–(12) in matrix form, we obtain

$$\mathbf{Q}_t + \mathbf{A}\mathbf{Q}_x + \mathbf{B}\mathbf{Q}_y = \mathbf{C}, \tag{13}$$

where

$$\mathbf{A} = \begin{pmatrix} u & 0 & \boxed{g} \\ 0 & u & 0 \\ \boxed{H} & 0 & u \end{pmatrix} \qquad \mathbf{B} = \begin{pmatrix} v & 0 & 0 \\ 0 & v & \boxed{g} \\ 0 & \boxed{H} & v \end{pmatrix}$$

$$\mathbf{Q} = \begin{pmatrix} u \\ v \\ \eta \end{pmatrix} \qquad \mathbf{C} = \begin{pmatrix} 0 \\ 0 \\ -uh_x - vh_y \end{pmatrix}.$$

Equation (13) is a strictly hyperbolic system with real and distinct eigenvalues. The characteristic equation, given by

$$det(q\mathbf{I} + r\mathbf{A} + s\mathbf{B}) = 0\,, \tag{14}$$

can be simplified as

$$(q + ru + sv)\left[(q + ru + sv)^2 - gH(r^2 + s^2)\right] = 0\,, \tag{15}$$

where the solution (r, s, q) of Eq. (15) are the directions normal to a characteristic cone at the cone's vertex. We split Eq. (15), whereby we obtain

$$q + ru + sv = 0$$

and

$$(q + ru + sv)^2 - gH(r^2 + s^2) = 0\,, \tag{16}$$

with the characteristic curves $u = dx/dt$ and $v = dy/dt$. If the characteristic cone has a vertex at $(\bar{x}, \bar{y}, \bar{t})$, then this cone consist of the line passing through vertex $(\bar{x}, \bar{y}, \bar{t})$ and parallel to the vector $(u, v, 1)$, satisfying

$$((x - \bar{x}) - u(t - \bar{t}))^2 + ((y - \bar{y}) - v(t - \bar{t}))^2 - gH(t - \bar{t})^2 = 0. \tag{17}$$

In particular, the gradient of the left hand side of (17) satisfies (16) on the cone surface. After solving (14), the solution yields

$$\lambda_1 = \boldsymbol{v} - \sqrt{gH}, \qquad \lambda_2 = \boldsymbol{v}, \qquad \lambda_3 = \boldsymbol{v} + \sqrt{gH}.$$

When the particle velocity $\boldsymbol{v}$ is far smaller than the particle celerity $\sqrt{gH}$, i.e., $|\boldsymbol{v}| \ll \sqrt{gH}$, the particle flow is said to be strictly subcritical and thus the characteristic speeds λ_1 and λ_3 have opposite directions. The maximum wave speed is given as

$$\lambda_{\max} = \max(\sqrt{gH_i}, \sqrt{gH_j}).$$

In this case, $\sqrt{gH}$ represents the dominant term which originates from the off diagonal terms g and H in the matrix $\mathbf{A}$ and $\mathbf{B}$.

We now have tracked back where the term $\sqrt{gH}$ originates from in the governing equations. We remark that the first part of the characteristic cone in (15) depends only on the particle velocity u and v. Equation (16), defining the second part of the characteristic cone, depends only on the celerity $\sqrt{gH}$. As we can see, gH in (15) comes from the off-diagonal terms g and H in the matrices $\mathbf{A}$ and $\mathbf{B}$. The terms g and H represent the coefficients of the derivative of the free surface elevation η_x in (10), the coefficient of the derivative η_y in (11) for the momentum equations, and the coefficient of velocity u_x and v_y in the volume conservation Eq. (12). We want to avoid the stability to depend on the celerity $\sqrt{gH}$, therefore we discretize the derivatives η_x, η_y and u_x, v_y implicitly.

Further along the lines of the above analysis, we now develop a semi-implicit SPH scheme for the two-dimensional shallow water equations. To this end, the derivatives of the free surface elevation η_x and η_y in the momentum equation and the derivative of the velocity in the continuity equation are discretized *implicitly*. The remaining terms, such as the nonlinear advective terms in the momentum equation, are discretized *explicitly*, so that the resulting equation system is linear.

Let us consider the continuity equation in the original conservative form, given as

$$\eta_t^n + \nabla \cdot (H^n \boldsymbol{v}^{n+1}) = 0.$$

The velocity $\mathbf{v}$ is discretized implicitly, whereas the total water depth H is discretized explicitly. In our following notation, for implicit and explicit discretization, we use $n+1$ and n for the superscript, respectively, i.e.,

$$\begin{aligned} \boldsymbol{v}_t^n + g \cdot \nabla \eta^{n+1} &= 0 \\ \eta_t^n + \nabla \cdot (H^n \boldsymbol{v}^{n+1}) &= 0. \end{aligned}$$

We discretize the particle velocities and free surface elevation in time by the Θ method, for the sake of time accuracy and computational efficiency, i.e., $n+1 = n+\Theta$, and so

$$\boldsymbol{v}_t^n + g \cdot \nabla \eta^{n+\Theta} = 0 \tag{18}$$

$$\eta_t^n + \nabla \cdot (H^n \boldsymbol{v}^{n+\Theta}) = 0 \tag{19}$$

where the Θ-method notation reads as

$$\begin{aligned} \eta^{n+\Theta} &= \Theta \eta^{n+1} + (1-\Theta)\eta^n \\ \boldsymbol{v}^{n+\Theta} &= \Theta \boldsymbol{v}^{n+1} + (1-\Theta)\boldsymbol{v}^n. \end{aligned}$$

The *implicitness factor* Θ should be in $[1/2, 1]$, according to Casulli and Cattani [5]. The general semi-implicit SPH discretization of (18)–(19) then takes the form

$$\frac{\boldsymbol{v}_{ij}^{n+1} - \boldsymbol{F}\boldsymbol{v}_{ij}^{n}}{\Delta t} + \frac{g}{\boldsymbol{\delta}_{ij}}\Theta(\eta_j^{n+1} - \eta_i^{n+1}) + \frac{g}{\boldsymbol{\delta}_{ij}}(1-\Theta)(\eta_j^{n} - \eta_i^{n}) = 0 \tag{20}$$

$$\begin{aligned}\frac{\eta_i^{n+1} - \eta_i^{n}}{\Delta t} &+ \Theta \sum_{j=1}^{N} \frac{m_j}{\rho_j}(2H_{ij}^{n}\boldsymbol{v}_{ij}^{n+1})\nabla \boldsymbol{W}_{ij} \cdot \boldsymbol{n}_{ij} \\ &+ (1-\Theta)\sum_{j=1}^{N} \frac{m_j}{\rho_j}(2H_{ij}^{n}\boldsymbol{v}_{ij}^{n})\nabla \boldsymbol{W}_{ij} \cdot \boldsymbol{n}_{ij} = 0\end{aligned} \tag{21}$$

where

$$H_{ij}^{n} = \max(0, h_{ij}^{n} + \eta_i^{n}, h_{ij}^{n} + \eta_j^{n}).$$

In a Lagrangian formulation, the explicit operator $\boldsymbol{F}\boldsymbol{v}_{ij}^{n}$ in (20) has the form

$$\mathbf{F}\mathbf{v}_{ij}^{n} = \frac{1}{2}(\mathbf{v}_i + \mathbf{v}_j),$$

where $\boldsymbol{v}_i$ and $\boldsymbol{v}_j$ denote the velocity of particles i and j at time t^n. The velocity at time t^{n+1} is obtained by summation,

$$\mathbf{v}_i^{n+1} = \mathbf{v}_i^{n} + \sum_{j=1}^{N} \frac{m_j}{\rho_j}(\mathbf{v}_{ij}^{n+1} - \mathbf{v}_i^{n})W_{ij}. \tag{22}$$

Note that in (20) we have *not* used the gradient of the kernel function for the discretization of the gradient of η. We rather used a finite difference discretization for the pressure gradient. This increases the accuracy, since $\boldsymbol{F}$ in (20) corresponds to an explicit spatial discretization of the advective terms. Since SPH is a Lagrangian scheme, the nonlinear convective term is discretized by the Lagrangian (material) derivative contained in the particle motion in (9). Equation (22) is used to interpolate the particle velocities from the particle location to the staggered velocity location.

3.5 The Free Surface Equation

Let the particle volume ω_i in (21) be given as $\omega_i = m_i/\rho_i$. Irrespective of the form imposed on $\boldsymbol{F}$, Eqs. (20)–(21) constitute a linear system of equations with unknowns $\boldsymbol{v}_i^{n+1}$ and η_i^{n+1} over the entire particle configuration. We solve this system at each time step for the particle variables from the prescribed initial and boundary conditions. To this end, the discrete momentum equation is substituted into the discrete continuity equation. This reduces the model to a smaller model, where η_i^{n+1} is the only unknown.

Multiplying (21) by ω_i and inserting (20) into (21), we obtain

$$\omega_i \eta_i^{n+1} - g\Theta^2 \frac{\Delta t^2}{\boldsymbol{\delta_{ij}}} \sum_{j=1}^{N} 2\omega_i\omega_j \left[H_{ij}^n (\eta_j^{n+1} - \eta_i^{n+1}) \nabla \boldsymbol{W}_{ij} \cdot \boldsymbol{n}_{ij} \right] = \boldsymbol{b}_i^n, \tag{23}$$

where the right hand side $\boldsymbol{b}_i^n$ represents the known values at time level t^n given as

$$\begin{aligned} \boldsymbol{b}_i^n &= \omega_i \eta_i^n - \Delta t \sum_{j=1}^{N} 2\omega_i\omega_j H_{ij}^n \boldsymbol{F}\boldsymbol{v}_{ij}^{n+\Theta} \nabla \boldsymbol{W}_{ij} \cdot \boldsymbol{n}_{ij} \\ &+ g\Theta(1-\Theta) \frac{\Delta t^2}{\boldsymbol{\delta_{ij}}} \sum_{j=1}^{N} 2\omega_i\omega_j \left[H_{ij}^n (\eta_j^n - \eta_i^n) \nabla \boldsymbol{W}_{ij} \cdot \boldsymbol{n}_{ij} \right], \end{aligned} \tag{24}$$

with $\boldsymbol{F}\boldsymbol{v}_{ij}^{n+\Theta} = \Theta \boldsymbol{F}\boldsymbol{v}_{ij}^n + (1-\Theta)\boldsymbol{v}_{ij}^n$. Since H_{ij}^n, ω_i, ω_j are non-negative numbers, Eqs. (23)–(24) constitute a linear system of N equations for η_i^{n+1} unknowns.

The resulting system is symmetric and positive definite. Therefore, the system has a unique solution, which can be computed efficiently by an iterative method. We obtain the new free surface location by (23), and (20) yields the particle velocity $\boldsymbol{v}_i^{n+1}$.

3.6 Neighboring Search Technique

The geometric search for neighboring particles j around a focal particle i at some specific position $\boldsymbol{x}_i$ can be done efficiently. To this end, we create a background Cartesian grid (see Fig. 3). This background grid contains the fluid with a mesh size of $2L$, and the grid is kept fixed throughout the simulation. The grid comprises macrocells which consist of particles (see [16] for computational details), quite similar to the book-keeping cells used in [14].

To compute the free surface elevation η and the fluid velocity $\boldsymbol{v}$, only particles inside the same macro cell or in the surrounding macro cells contribute. Ferarri et al. [9] explain the neighboring search in detail: The idea is to build a list of particles in a given macro cell and, vice versa, to keep a list of indices, one for each particle, pointing to macro cells containing that particle. We store the coordinates of each particle to reduce the time required for the neighbor search. In our neighbor search,

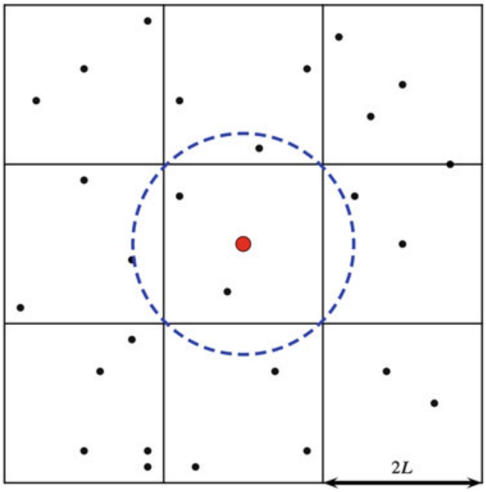

Fig. 3 Fictitious Cartesian grid: neighboring search is done within the nine cells in a two-dimensional space. The smoothing length is constant and the support domain for the particles is $2L$

a particle can only interact with particles in its macro cell or in neighboring macro cells. For the two-dimensional case of the present study we only need to loop over the bounding box of nine macro cells (see Fig. 3).

4 Numerical Results

Now we evaluate the performance of the proposed semi-implicit SPH scheme. This is done by employing a standard test problem for the 2d shallow water equations. In this model problem, we assume a smooth solution, i.e., a collapsing Gaussian bump.

4.1 A Collapsing Gaussian Bump

We consider a smooth free surface wave propagation, by the initial value problem

$$\eta(x, y, 0) = 1 + 0.1e^{-\frac{1}{2}\left(\frac{r^2}{\sigma^2}\right)},$$
$$u(x, y, 0) = v(x, y, 0) = h(x, y) = 0,$$

in the domain $\Omega = [-1, 1] \times [-1, 1]$ with a prescribed flat bottom bathymetry, i.e., $h(x, y) = 0$, where $\sigma = 0.1$ and $r^2 = x^2 + y^2$. The computational domain Ω is discretized with 124,980 particles. The final simulation time is $t = 0.15$, and the time step is chosen to be $\Delta t = 0.0015$. We have used the implicitness factor $\Theta =$

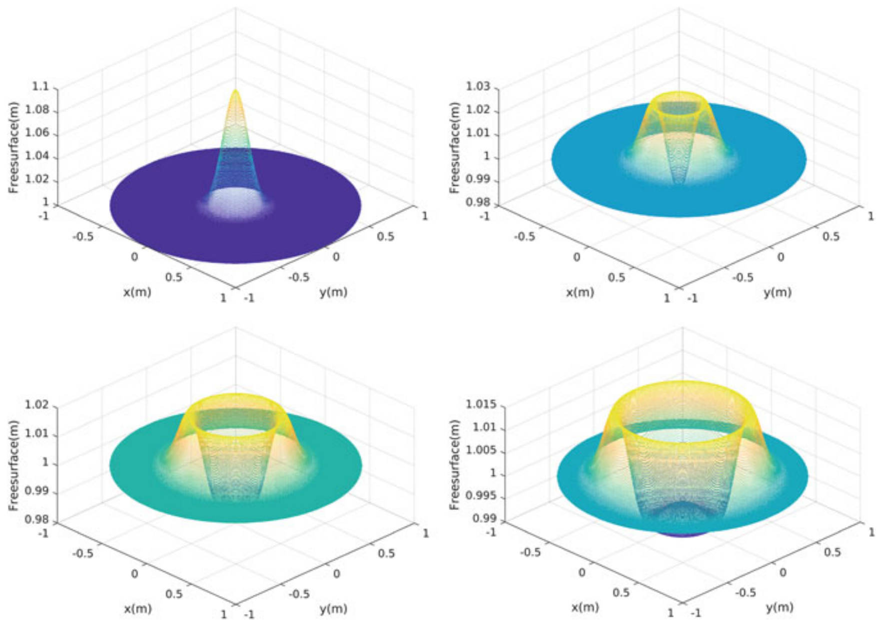

Fig. 4 3d surface plot of the free-surface: SISPH solution at times t =0.0 s, 0.05 s, 0.10 s, 0.15 s with 124,980 particles

0.65. The smoothing length is taken as $h_i = \alpha(\omega_i)^{1/d}$, where $\alpha = [1.5, 2]$ and $d = 2$. The obtained numerical solution is shown in Fig. 5. The profiles in Fig. 4 show the three dimensional surface plots of the free surface elevation at times t =0.0 s, 0.05 s, 0.10 s, 0.15 s. Due to the radial symmetry of the problem, we obtain a reference solution by solving the one-dimensional shallow water equations with a geometric source term in radial direction: a method based on the high order classical shock capturing total variation diminishing (TVD) finite volume scheme is employed for computing the reference solution using 5000 points and the Osher-type flux for the Riemann solver, see [20] for details. The comparison between our numerical results obtained with semi-implicit SPH scheme and the reference solution is shown. A good agreement between the two solutions is observed in Fig. 5. We attribute the (rather small) differences in the plots to the fact that the SPH method has a larger effective stencil, which may increase the numerical viscosity. The cross section of the free surface elevation and the velocity in the x-direction is shown in Fig. 5. We have used a higher resolution of particle numbers of 195,496, the cross section of the free surface elevation and the velocity at final time $t = 0.15$ s can be seen in Fig. 6. We observe similar results compared to particle numbers 124,980.

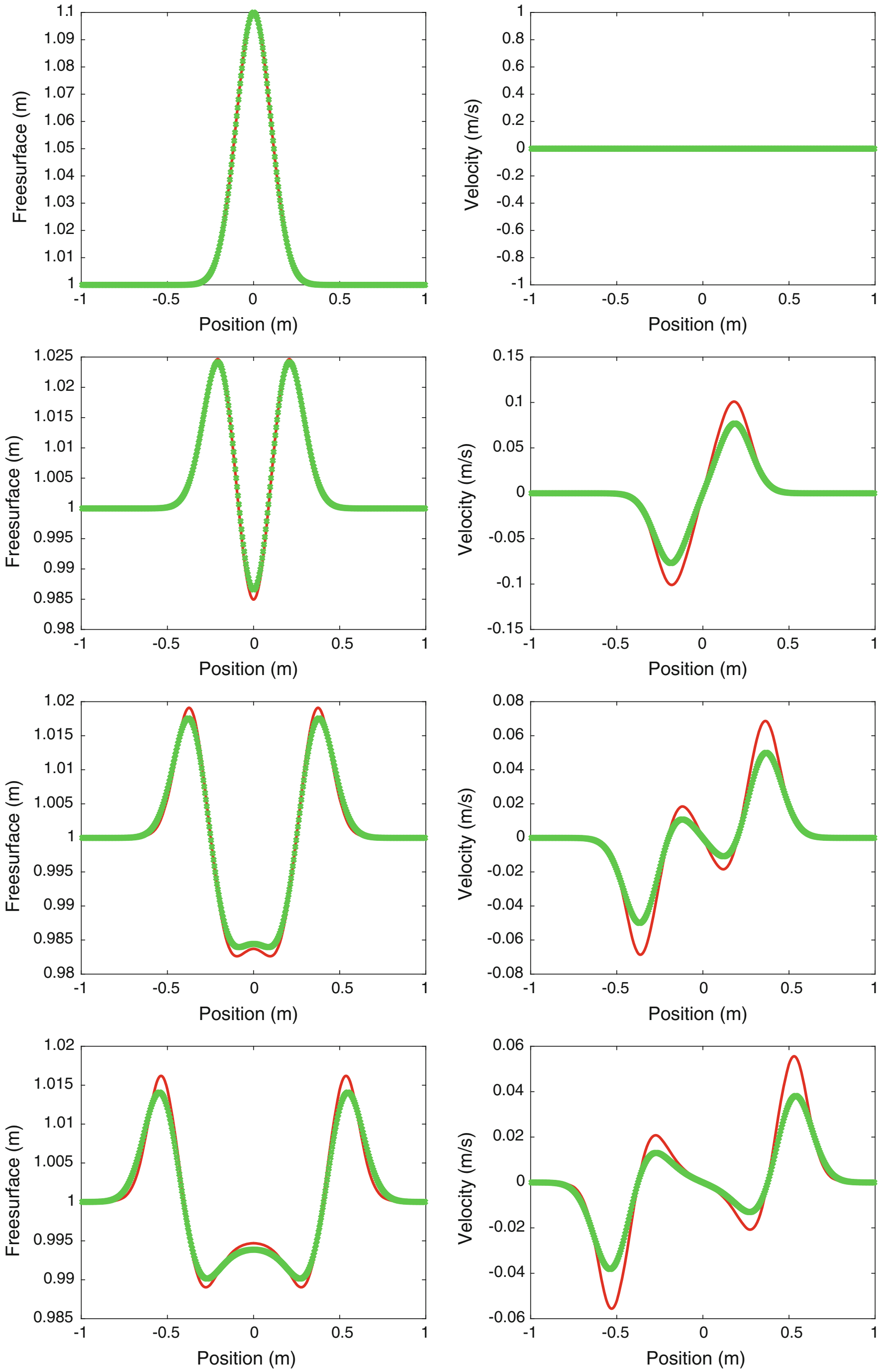

Fig. 5 Cross section of semi-implicit solution (*green*) versus reference solution (*red*): Free-surface (*left*), velocity (*right*) in the x-direction at times $t = 0.0$ s, 0.05 s, 0.10 s, 0.15 s

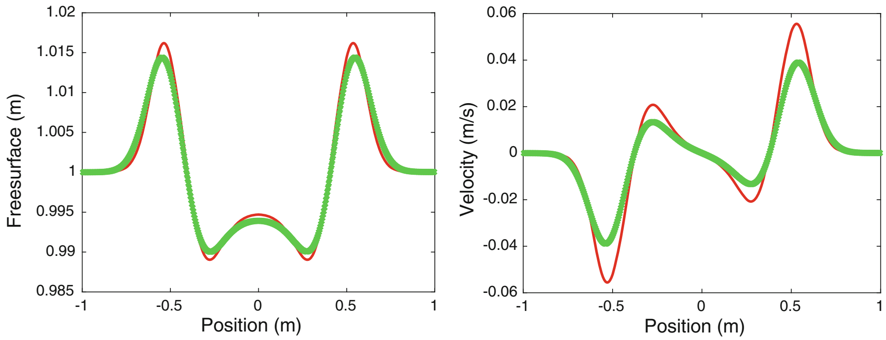

Fig. 6 Cross section of semi-implicit solution (*green*) versus reference solution (*red*): Free-surface (*left*), velocity (*right*) in the x-direction at times $t = 0.15$ s with a higher resolution of 195,496 particles

5 Conclusion

We have proposed a meshfree semi-implicit smoothed particle hydrodynamics (SPH) method for the shallow water equations in two space dimensions. In our scheme, the momentum equation is discretized by a finite difference approximation for the gradient of the free surface and the SPH approximation for the mass conservation equation. By the substitution of the discrete momentum equations into the discrete mass conservation equations, this leads to a sparse linear system for the free surface elevation. We solve this system efficiently by a matrix-free version of the conjugate gradient (CG) algorithm.

The key features of the proposed semi-implicit SPH method are briefly as follows: The method is mass conservative; efficient; time steps are not restricted by a stability condition (coupled to the surface wave speed), thus large time steps are permitted.

Ongoing research is devoted to nonlinear wetting and drying problems, application to shock problems, and extension of the scheme to the fully three-dimensional case.

References

1. T. Belytschko, Y. Krongauz, J. Dolbow, C. Gerlach, On the completeness of meshfree particle methods. Int. J. Numer. Meth. Eng. **43**(5), 785–819 (1998)
2. B. Ben Moussa, J.P. Villa, Convergence of SPH method for scalar nonlinear conservation laws. SIAM J. Numer. Anal. **37**(3), 863–887 (2000)
3. L. Bonaventura, A. Iske, E. Miglio, Kernel-based vector field reconstruction in computational fluid dynamic models. Int. J. Numer. Methods Fluids **66**(6), 714–729 (2011)
4. V. Casulli, Semi-implicit finite difference methods for the two-dimensional shallow water equations. J. Comput. Phys. **86**, 56–74 (1990)

5. V. Casulli, E. Cattani, Stability, accuracy and efficiency of a semi-implicit method for three-dimensional shallow water flow. Comput. Math. Appl. **27**(4), 99–112 (1994)
6. V. Casulli, R.T. Cheng, Semi-implicit finite difference methods for the three-dimensional shallow water flows. Int. J. Numer. Methods Fluids **15**, 629–648 (1992)
7. V. Casulli, R.A. Walters, An unstructured grid, three-dimensional model based on the shallow water equations. Int. J. Numer. Methods Fluids **32**, 331–348 (2000)
8. M. Dumbser, V. Casulli, A staggered semi-implicit spectral discontinuous Galerkin scheme for the shallow water equations. Appl. Math. Comput. **219**, 8057–8077 (2013)
9. A. Ferarri, M. Dumbser, E.F. Toro, A. Armanini, A new 3d parallel SPH scheme for free surface flows. Comput. Fluid **38**(6), 1203–1217 (2009)
10. R.A. Gingold, J.J. Monaghan, Smoothed particle hydrodynamics – theory and application to non-spherical stars. Mon. Not. Roy. Astron. Soc. **181**, 375–389 (1977)
11. G.H. Golub, C.F. van Loan, *Matrix Computations*, 3rd edn. (J. Hopkins, London, 1996)
12. A. Iske, M. Käser, Conservative semi-Lagrangian advection on adaptive unstructured meshes. Numer. Methods Partial Differ. Equ. **20**(3), 388–411 (2004)
13. M. Lentine, J.T. Gretarsson, R. Fedkiw, An unconditionally stable fully conservative semi-Lagrangian method. J. Comput. Phys. **230**(8), 2857–2879 (2011)
14. J.J. Monaghan, Simulating free surface flows with SPH. J. Comput. Phys. **110**, 399–406 (1994)
15. J.J. Monaghan, Smoothed particle hydrodynamics. Rep. Progr. Phys. **68**, 1703–1759 (2005)
16. J.J. Monaghan, J.C. Lattanzio, A refined particle method for astrophysical problems. Astron. Astrophys. **149**, 135–143 (1985)
17. Y. Saad, *Iterative Methods for Sparse Linear Systems*, 2nd edn. (SIAM, Philadelphia, 2003)
18. D. Shepard, A two dimensional interpolation function for irregular spaced data. *Proceedings of the 23rd A.C.M. National Conference* (1968), pp. 517–524
19. M. Tavelli, M. Dumbser, A high order semi-implicit discontinuous Galerkin method for the two dimensional shallow water equations on staggered unstructured meshes. Appl. Math. Comput. **234**, 623–644 (2014)
20. E.F. Toro, *Shock-Capturing Methods for Free-Surface Shallow Flows*, 2nd edn. (Wiley, Chichester, 2001)
21. J.P. Villa, On particle weighted methods and smooth particle hydrodynamics. Math. Models Methods Appl. Sci. **9**(2),161–209 (1999)